AN ECLOGITISED OCEANIC PALAEO-HYDROTHERMAL FIELD FROM THE ST. MARCEL VALLEY (ITALIAN WESTERN ALPS)

Silvana Martin*, Gisella Rebay✉, Jean-Robert Kienast***** and **Catherine Mével*****

* *Dipartimento di Scienze Chimiche e Ambientali, Università dell'Insubria, Como, Italy.*
** *Dipartimento di Scienze della Terra, Università di Pavia, Italy.*
*** *Laboratoire de Geosciences Marines, IPGP, Université Paris VII, France.*
✉ *Corresponding author, e-mail: rebay@crystal.unipv.it*

Keywords: *Eclogitic ophiolite, Mg-Fe hydrothermal metamorphosed rocks, oceanic alteration, pseudosections, Servette ore deposit. Western Alps, Italy.*

ABSTRACT

The eclogite-facies Servette metaophiolites (St. Marcel Valley, Italian Western Alps) belong to the Piedmont Nappe. They are glaucophanite, chloriteschists, talcschists and associated mineralised quartzite derived from different types of hydrated Tethyan oceanic crust affected by sea-floor and sub-sea floor hydrothermal alteration. We first describe the geology and lithology of the Servette metaophiolites and their chemical signature, and then we focus on the estimation of the Alpine subduction-related peak P-T metamorphic conditions and associated microstructures. Estimation of the peak P-T conditions was performed via calculations of pseudosections representing the equilibrium assemblages in the studied rocks using THERMOCALC. These calculations yielded relatively uniform values for the high-pressure metamorphic equilibration, with temperatures of 550 ± 60°C and pressures of 2.1 ± 0.3 Gpa, higher than the previously estimated P-T in the St. Marcel Valley (T max = 500°C and P max = 1.4 GPa), but lower than those obtained in other localities of the Zermatt-Saas zone (T up to 550-600° C and P up to 2.5-3.0 GPa). Comparison with similar rocks from the Zermatt-Saas zone helps to constrain the peculiar conditions at the P peak of these hydrated rocks within the Alpine subduction slab.

INTRODUCTION

The Western Alps retain composite km-scale relics of the Mesozoic Tethys oceanic lithosphere. They correspond to the well known "ophiolites", first defined by Brongniart (1813) (which have been interpreted as derived from an oceanic lithosphere only since the advent of the plate tectonics, Gass, 1968). Ophiolites include rocks derived from different parts of the oceanic litosphere (see Bernoulli et al., 2003, for the origin of ophiolites and the related concept).

In this paper we focus on peculiar rocks derived from parts of the oceanic crust which suffered extreme hydration and hydrothermal alteration, usually located at the mid-ocean ridge (e.g., Bonatti et al., 1976). Because of extreme hydration, these rocks changed their original chemistry acquiring special whole rock compositions which strongly influenced the mineralogy of the high pressure subduction assemblages and the isotope composition, as observed in the metaophiolites of the Piedmont Nappe (Barnicoat and Bowtell, 1995; Cartwright and Barnicoat, 1999; Miller and Cartwright, 2000). The metaophiolites preserve trace of their peculiar oceanic compositions in spite of the subduction metamorphism and the orogenic deformations that they underwent (e.g., Venturelli et al., 1981; Beccaluva et al., 1984; Pfeifer et al., 1989; Cartwright and Barnicoat, 1999; Widmer et al., 2000; Martin and Cortiana, 2001).

Advances have been made in the study of hydrothermal alteration in mafic rocks and sediments from present-day mid-ocean ridges (Alt and Honnorez, 1984; Alt et al., 1986; Pineau et al., 1976; Lowell et al., 1995; Miller and Cartwright, 2000). Other data come from the Fe-Cu-Zn and Mn mineralisations associated either with unmetamorphosed ophiolites in the Apennines (e.g., Cortesogno et al., 1979) or with metamorphosed ophiolites in the Alps (e.g., Debenedetti, 1965; Martin-Vernizzi, 1982; Mottana, 1986) and in the Aegean Islands (Reinecke, 1982). However, finding a complete oceanic crustal section in ophiolites including serpentinites, gabbros, sheeted dykes, pillow lavas and manganiferous cherts is an exception (e.g., Debenedetti, 1965; Martin et al., 1994; Miller and Cartwright, 2000).

A well-known eclogitised section of the Mesozoic Tethys ocean floor that suffered extreme hydrothermal alteration crops out in the St. Marcel Valley (Castello, 1981; Martin-Vernizzi, 1982; Cartwright and Barnicoat, 1999; Martin et al., 2004). Here hydrothermal Fe-Cu sulphide bearing mineralisations occur at Servette and Chuc; a Mn-deposit is present in the nearby Praborna and in other sites of the valley (Castello, 1981).

The earliest studies on the St. Marcel rocks have been focussed on the Praborna deposit due to the presence of wonderful coloured Mn-minerals (e.g., Brown et al., 1978; Griffin and Mottana, 1982; Martin-Vernizzi, 1982; Kienast e Martin, 1983; Martin and Kienast, 1987; Perseil, 1988; Perseil and Smith, 1995; Tumiati, 2005). Further studies addressed the geological setting of the St. Marcel Valley (Castello et al., 1980; Tartarotti et al., 1986; Tartarotti, 1988; Martin and Tartarotti, 1989), the Servette ore deposit (Natale, 1966; Dal Piaz and Omenetto, 1978; Castello, 1981), the bulk-rock and mineral chemistry (Krutow-Mozgawa, 1988), trace element trends of the metabasites (Barnicoat and Bowtell, 1995), oxygen isotopes (Cartwright and Barnicoat, 1999) and age determination (Dal Piaz et al., 2001). All these studies established that the protolith of these rocks was a piece of oceanic crust in which hydrothermal alteration took place during ocean-floor formation. The oceanic hydrothermal activity is confirmed by the occurrence of the hydrothermal sulphide and Mn ore deposits.

In this paper we describe the high pressure rocks from Servette and concentrate on their mineral assemblages in order to unravel the influence of the original chemistry on the mineral crystallization during Alpine metamorphism and to quantify the peak metamorphic conditions at which they formed.

GEOLOGICAL SETTING

The St. Marcel metaophiolites are part of the Piedmont Nappe of the Western Alps. They overlie the Gran Paradiso basement nappe and are overthrust by the Austroalpine Mt. Emilius klippe (Fig. 1). The St. Marcel metaophiolites belong to the 150 km^2 wide Mt. Avic complex (Zermatt-Saas zone) at the southern side of the Aosta Valley. Its eastern portion includes a large body of serpentinized peridotite (Mt. Avic Massif), metagabbro bodies (e.g., Mt. Barbeston), chloriteschists, talcschists, glaucophanite and minor quartzite, micaschists and calcschists.

The metaophiolites exposed in the lower St. Marcel Valley, beneath the northern termination of the Mt. Emilius Austroalpine klippe, consist of two slices, from top to bottom (Fig. 2a and 2b): (i) the Mt. Roux slice, including strongly deformed greenschists (prasinite *auct.,)*, serpentinite, retrogressed metagabbro with rare eclogite relics; and (ii) the Servette slice, made of dominant glaucophanite and metasediments with eclogitic fabric and parageneses (Fig. 2). The intensity of the retrograde greenschist facies overprint and deformation decreases from top (near the tectonic contact with the Mt. Emilius klippe) to bottom of the metaophiolite.

A mylonitic serpentinite sliver occurs between the metaophiolites and the overlying Mt. Emilius klippe; other mylonitic serpentinites are located between the Mt. Roux slice and the underlying Servette slice (Fig. 2b).

The uppermost section of the Servette slice consists of interlayered glaucophanite, chloriteschists, talcschists, boudins of fine-grained eclogite, clinopyroxenite and eclogite-facies metagabbro, minor quartzite and metasomatic rocks (Tartarotti, 1988; Tartarotti and Caucia, 1993). This section is well exposed on the eastern side of the lower St. Marcel Valley between the Fontillon Damon ridge and the Servette mine (Fig. 2a and 2b)

The interlayering of glaucophanite (about 50%), chloriteschists (20%), talcschists (15%), quartzite (10%) and minor eclogite (5%) in the Servette slice has been interpreted as resulting from deformation under high-pressure metamorphic conditions of mafic and ultramafic materials and quartz-bearing sediments (Martin and Tartarotti, 1989). However, on the basis of other studies on this slice and on similar rock complexes (Bearth, 1967; Ernst and Dal Piaz, 1978; Krutow-Mozgawa, 1988; Barnicoat and Botwell, 1995; Widmer et al., 2000), the mafic interlayering seems to be derived from both tectonic transposition and different chemical compositions related to variable degrees of oceanic hydrothermal alteration of mafic MOR material (see Alt and Honnorez, 1984, for alteration of present-day oceanic crust; see also Bucher et al., 2005). In particular, the talcschists of Servette could be compared with chloritoid-garnet-talc eclogitic rocks from Pfulwepass (Zermatt-Saas zone), interpreted as derived from chloritised metasomatites (Widmer et al., 2000).

The uppermost section of the Servette slice (Fig. 2) includes the Cu-Fe sulphide ore deposits of Chuc and Servette. The Servette mineralisation is concentrated in two major ENE-dipping layers of 3-4 m in thickness, located at the boundary between chloriteschists and glaucophanite, and some minor levels (less than 1 m) within the chloriteschists (Fig. 2b and 2c) (Martin et al., 2004, and ref. therein). The Chuc ore deposit has a similar setting , but it is located in the glaucophanite beneath Mt. Emilius on the left side of the valley (Castello, 1981). Primary sulphides (pyrite, chalcopyrite, sphalerite, pyrrotine, bornite, neodigenite, marcassite, mackinawite and native Cu) and oxides (rutile, ilmenite, hematite and magnetite) are present in massive lenses and disseminated in the rocks (Jervis, 1873; Moretti, 1948; Bearth, 1967; Natale, 1969; GLOM, 1977; Cesti, 1978; Dal Piaz and Omenetto, 1978; Castello et al., 1980; Martin et al., 2004; Tumiati et al., 2005).

The Servette mineralisation is overlain by Mn-rich quartzite grading upwards into carbonate-rich micaschists and calcschists (level 1818 m, in Fig. 2b). A metasomatic layer (up to 5-8 m thick) separates these metasedimentary rocks from mylonitic serpentinite at the base of the Mt. Roux slice (Fig. 2b).

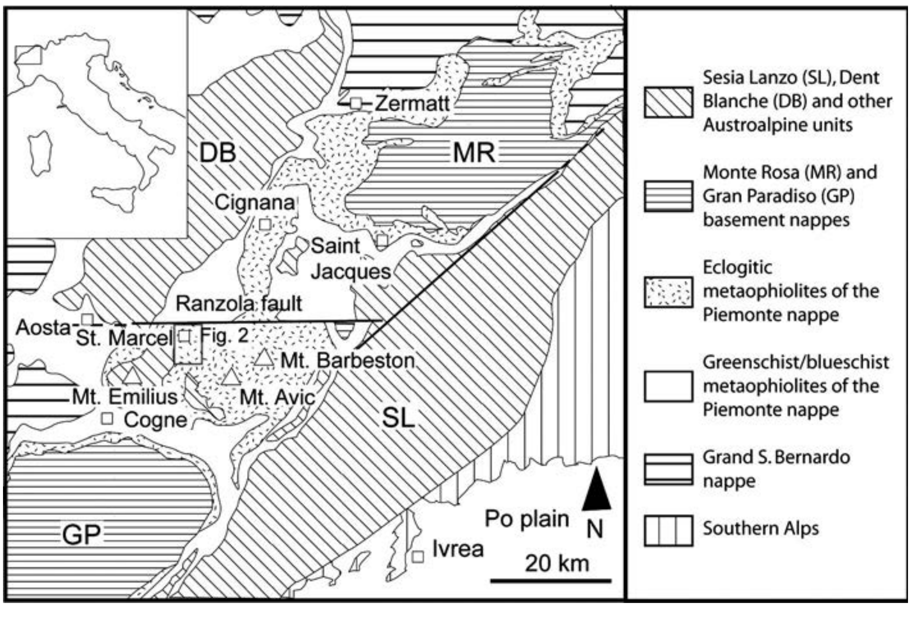

Fig. 1 - Tectonic sketch map of the Aosta Valley and location of the St. Marcel Valley.

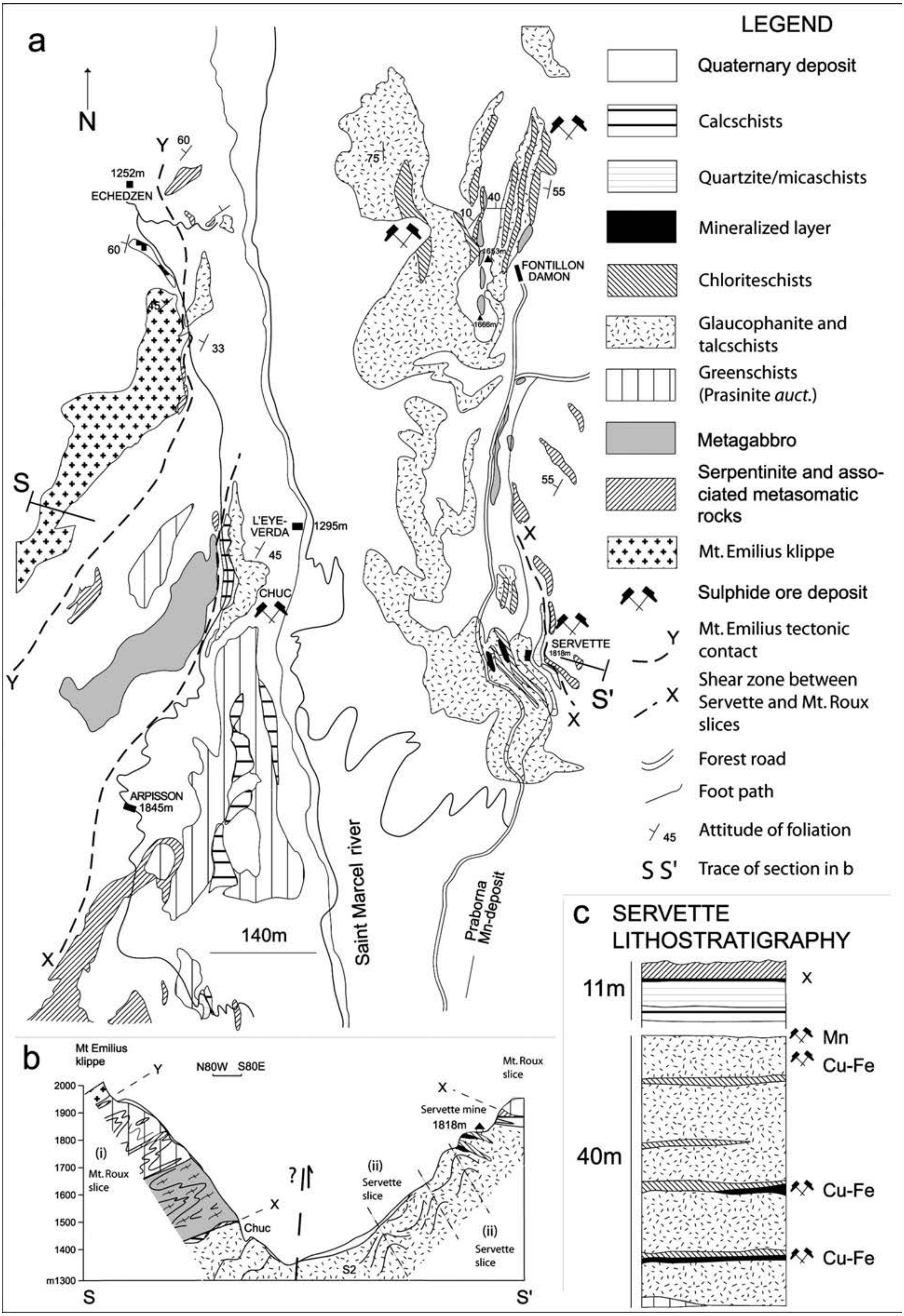

Fig. 2 - (a) Geological map of the lower St. Marcel Valley. Y- tectonic boundary of the metaophiolites with the overlying Mt. Emilius Austroalpine klippe; X- internal contact between the Mt. Roux and Servette metaophiolite slices. (b) Schematic geological section across the valley [S-S' in (a)]; (c) lithostratigraphy of the Servette ore deposit.

The Servette and Mt. Roux slices show four phases of mesoscale deformation. The earliest one produced a rarely preserved prograde S_1 foliation. This was later deformed by a D_2 deformation, having a mylonitic character as indicated by the N-S trending lineated glaucophane and by the sheared garnets.

The S_2 foliation strikes N-S and dips 60° - 80° West and includes some eclogite boudins on the Fontillon Damon ridge (Servette slice, in Fig. 2; Martin and Tartarotti, 1989). Microstructural relics of the earliest D_1 deformation event have been recognized in the core of zoned centimetre-sized garnets of the glaucophanite; these relics are absent in the matrix due to the D_2 mylonitic deformation.

The S_2 foliation was superimposed by a later deformation phase (D_3) characterized by folds with N-S axes, with 20° to 60° steep E-dipping axial planes associated to greenschist-facies retrogression (Fig. 2). This retrogression is mostly widespread in the metagabbro and greenschists of the Mt. Roux slice, on the western side of the St. Marcel Valley, below the Mt. Emilius klippe. A later deformation phase D_4, associated with increasing retrogression, is marked by E-W trending axes (Tartarotti, 1988). South dipping E-W fault planes, developed at Servette (Roman mine, Martin et al., 2004), belong to the brittle Aosta-Ranzola fault system (Fig. 1).

The Servette slice underwent a polymetamorphic evolution from an oceanic hydrothermal alteration stage, through a prograde blueschist-facies, to a peak eclogite-facies metamorphism at 550°C and 1.0-1.5 GPa (Martin and Tartarotti, 1989) of Eocene age (45±2.8, Rb/Sr age on phengitic Mn-mica, and 44-47±1.5 Ma, $^{40}Ar/^{39}Ar$ age, calculated for white micas from the Servette Mn-rich quartzite: Dal Piaz et al., 2001). A new determination of the Eocene P-T peak conditions is one of the aims of this work.

A lithological affinity between the St. Marcel and the Valtournanche metaophiolites, these latter associated to coesite-bearing Mn-quartzite (Reinecke, 1998), was pointed out by Dal Piaz (1999, and ref. therein). However, until now, no proof of very high pressure, coesite-bearing eclogite-peak conditions has yet been given for the St. Marcel metaophiolites.

LITHOLOGIES AND BULK COMPOSITION

Three groups of mafic lithologies were selected for detailed descriptions and analyses, i.e. chloriteschists, talcschists and glaucophanite of the Servette slice, characterized by different silica content and hydrated mineral assemblages. Description of the remaining lithologies (see Fig. 2) is given in Tartarotti et al. (1986) and Martin and Tartarotti (1989). The chemistry of these "blueschist rocks" is discussed at the end of this chapter to explain their peculiar mineralogical composition (Table 1).

Chloriteschists

Chloriteschists have dominant chlorite and minor garnet (Fig. 3a), quartz, talc, chloritoid, sodic amphibole ("crossite"), ± paragonite and accessory sulphides, rutile, epidote, ilmenite, all of which are aligned along the main foliation. These rocks display two foliations outlined by flakes of chlorite: a main foliation plane (the prograde S_1 foliation) and a C-plane (shear plane), intersecting each other at about 35°. The C-planes coincide with the mylonitic foliation of the associated glaucophanite. Garnet occurs as zoned euhedral porphyroblasts up to 1 cm in diameter, including titanite, apatite, quartz and sodic amphibole at the core, and rutile, ilmenite and chloritoid at the rim. The core inclusions outline the trace of a prograde (S_1) foliation. Chloritoid forms cm-sized porphyroblasts elongated along the main foliation and stretched clasts along the C-planes; sometimes it may include sodic amphibole. It is often replaced by secondary chlorite, but may recrystallize as new grains at the boundary of the earliest large porphyroblasts. Rare sodic amphibole ("crossite") crystals show rims of blue-green secondary hornblende. Quartz and albite form polycrystalline aggregates within the chlorite matrix.

Sample MJ13 (Fig. 3b) has been selected as the most representative chloriteschist. Besides the chlorite matrix and chloritoid and garnet porphyroblasts, it contains minor talc, sodic amphibole ("crossite"), ilmenite, allanite, pyrite and chalcopyrite. Secondary chlorite crystallizes along fractures in garnet and around garnet and chloritoid. Garnet is zoned, with pinkish core and reddish, regular and sharp rims with chloritoid inclusions near the rims (Fig. 3b). Chloritoids aligned along the mylonitic foliation are retrogressed to paragonite (not abundant) and chlorite.

Talcschists

In the talcschists (Fig 3c), centimetre-sized zoned garnets and large (up to 5 cm long) chloritoid porphyroblasts are embedded in a fine-grained, talc-dominated matrix (Fig. 3c and d). Titanite and quartz occur as inclusions in the core of garnets, whereas chloritoid and talc, along with rutile and quartz, occur in the rim of garnets. Secondary, retrograde talc is sometimes observed in veins crosscutting the main foliation. Talcschists are locally interlayered with quartz-rich layers. Garnet and sulphide preserving prograde cummingtonite and sodic amphibole inclusions are found.

Sample MJ23 is composed of millimetric layers of talc and quartz, defining the main foliation. Garnet, glaucophane, chloritoid and sulphides are irregularly disseminated in the matrix. In the talc-rich layers, talc coexists with garnet, rutile and chloritoid (Fig. 3d). Zoned garnet includes epidote and titanite at the core, and talc at the rim. Small (1 mm) euhedral clear garnets occur in the quartz-rich layers.

Table 1 - Summary of assemblages observed in different lithologies.

Rock	Chloriteschists	Talcschists	Glaucophanite
Prograde (S1)	chlorite, garnet, sodic amphibole, titanite, apatite, quartz, pyrite, allanite	talc, garnet, quartz, epidote, titanite, sulphide, magnetite	glaucophane, lawsonite, garnet, titanite, apatite, clinozoisite, quartz
Peak (S2)	chlorite, garnet, chloritoid, sodic amphibole, talc, rutile, sulphide	talc, chloritoid, garnet, rutile, sulphide, glaucophane, quartz	glaucophane, garnet, chloritoid, phengite, clinozoisite, talc, rutile, quartz
Retrograde (S3 and pseudomorphs)	chlorite, chloritoid, paragonite, blue green hornblende, talc, ilmenite, quartz, albite, sulphide	chlorite, paragonite, talc, ilmenite, sulphide	paragonite, talc, albite, chlorite, magnetite, ilmenite, blue-green hornblende, clinozoisite, sulphide

Chloritoid can be completely consumed to produce chlorite + paragonite rims, caused by the retrograde reaction chloritoid + glaucophane+talc = chlorite + paragonite. Glaucophane is rare and not retrograded.

Glaucophanite

Glaucophanite (Fig. 3e and f) is composed of glaucophane, garnet, chloritoid, clinozoisite/epidote, paragonite, talc and accessory phengite, rutile, magnetite and ilmenite. Glaucophane is strongly aligned in the main foliation and is

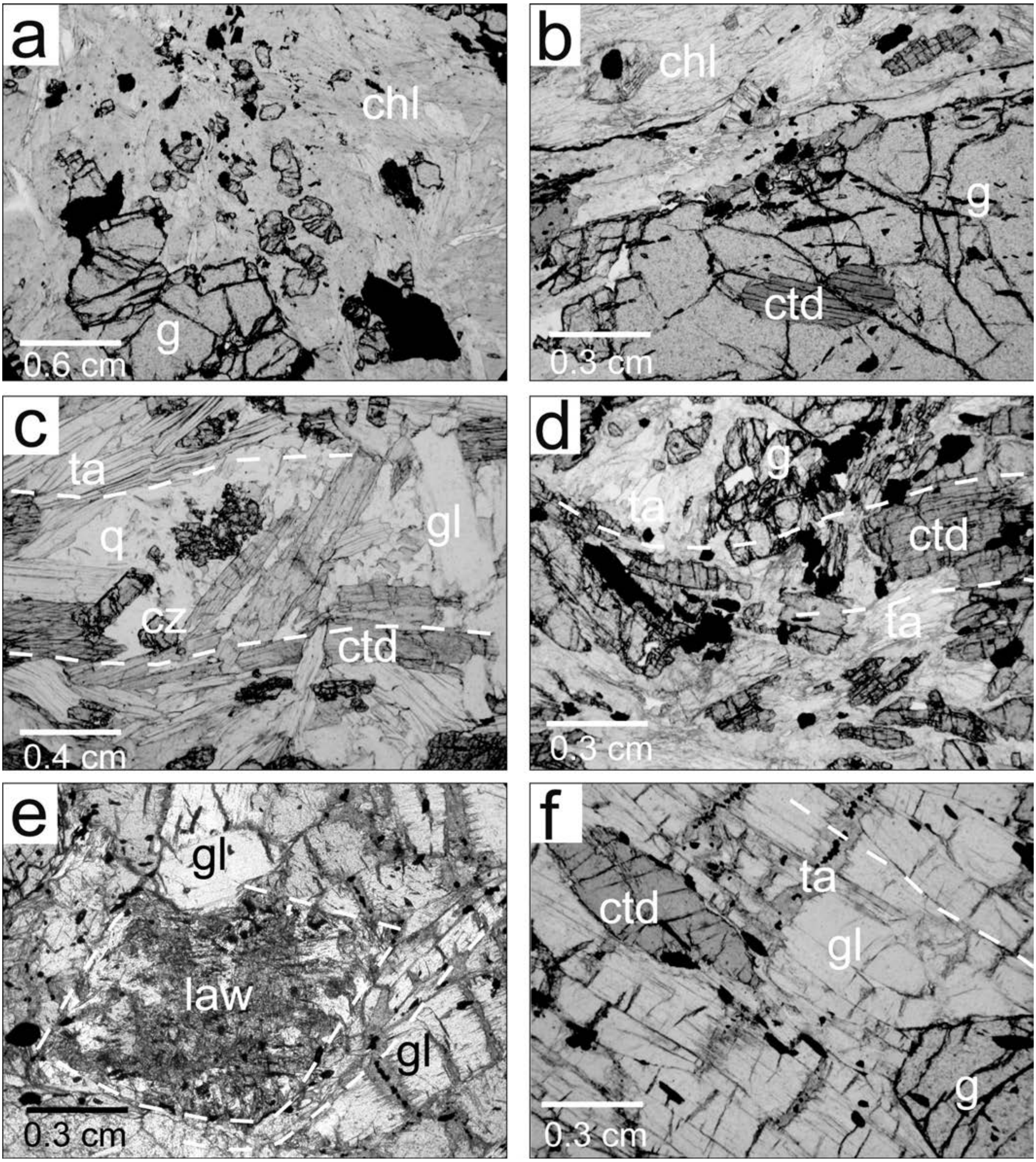

Fig. 3 - Photomicrographs of the Servette rocks. *Chloriteschists*: a) hypidiomorphic large and small garnets (g) and magnetite (black) in a chlorite (chl) matrix; b) portion of a large garnet with chloritoid inclusions in the rim, and partially retrograded chloritoid (ctd) in the chlorite (chl) matrix. *Talcschists*: c) Talc (ta), glaucophane (gl), chloritoid (ctd), clinozoisite (cz) and quartz (q); d) Chloritoid (ctd), talc (ta), garnet (g) and magnetite (black) all aligned in the main foliation. *Glaucophanite*: e) pseudomorphs after lawsonite (law). The aggregate is mainly made of paragonite and epidote. Glaucophane (gl) is also indicated; f) garnet (g), glaucophane (gl) and chloritoid (ctd) aligned along the main foliation. Glaucophane is stretched and veins are filled with talc (ta) and magnetite (black). White broken lines represent orientation of the main foliation.

microboudinaged parallel to the N-S trending lineation. Secondary talc, magnetite, albite and paragonite aggregates fill the stretching-related fractures; glaucophane is rimmed by blue-green secondary amphibole (Fig. 3e and f).

Garnets occur with different sizes: large (up to 5 mm in diameter) zoned crystals and small (1 mm) clear garnets. Large garnets can be strongly deformed to assume a sigmoidal shape and boudinaged with fractures at the neck of boudins filled by glaucophane. The large garnets are porphyroblasts with the core including quartz and titanite, the inner rim including rutile, quartz, chloritoid, pseudomorphs after lawsonite, ilmenite and glaucophane syn-kynematic with D_2 deformation, and a clear and statically crystallized external rim. In the outermost rim, which cuts the external foliation, inclusions are generally absent. All the inclusions are represented by single grain minerals, and they are not connected to the matrix by cracks and fractures. Small garnets that occur in the matrix appear unzoned, unaltered and syn-kinematic with the D_2 shearing deformation.

Lozenge-shaped aggregates consisting of zoisite, and/or clinozoisite, paragonite, calcite, albite and chlorite enclosed in the garnet or in the matrix are interpreted as pseudomorphs after prograde lawsonite. The pseudomorphs in the matrix are often sigmoidal due to the D_2 shearing deformation.

Glaucophanite in contact with talcschists is generally characterized by the absence of pseudomorphs after lawsonite, abundance of glaucophane and small garnets, whereas the associated talcschists have abundant talc and large garnets. In both rocks chloritoid is up to 3-4 cm in length; it has no inclusions, especially when in contact with quartz (Fig. 3b and c). Glaucophanite in contact with chloriteschists shows numerous chloritoid- and chlorite-rich levels. Chloritoid occurs as mm-to-cm porphyroblasts, that are often strongly deformed, kinked and with sigmoidal shape.

Sample MJ20 has a matrix composed of glaucophane, talc, chlorite and accessory rutile and apatite, with well preserved pseudomorphs after lawsonite consisting of zoisite, clinozoisite, paragonite, phengite and quartz (Fig. 3e), large crystals of chloritoid and rare small garnets elongated in the foliation (Fig. 3f). Chloritoid is replaced by chlorite and paragonite. Glaucophane is replaced by blue-green hornblende at the rims.

Bulk rock composition

Bulk rock composition of the analysed samples plot in two main fields in the AFM diagram (Fig. 4). The St. Marcel glaucophanite compositions plot in the same field of the Zermatt-Saas metaophiolites and of other metabasites of the Piemonte Nappe (Fig. 4a, Table 2) (Dal Piaz and Ernst, 1978; Dal Piaz et al., 1981; Beccaluva et al., 1984; Widmer et al., 2000; Bocchio et al., 2000; Martin and Cortiana, 2001). They follow a typical MORB differentiation trend, although they display an enrichment in alkalies possibly due to oceanic spilitisation (see Nakamura et al., 2007). Their compositional scattering is due to hydrothermal alteration, depending on temperature, chemistry of fluids (pH; element concentration) and rock/sea water ratio (e.g. Knott et al., 1998; Honnorez et al., 1998).

Glaucophanites MJ20 and MJ22 from Servette are enriched in Cr (403, 291 ppm respectively), V (234, 323 ppm), Zr (93, 154 ppm; Table 2) and could derive from a hydrated mixture of gabbro and basalt, as suggested for some Queyras metaophiolites by Lagabrielle and Cotten (1984).

The Servette chloriteschists and talcschists plot along the FM tie-line (Fig. 4a), due to a peculiar low content of alkalies. Chloriteschists MJ12 and MJ13 are depleted in SiO_2 (24.74, 23.92 wt%) and enriched in FeO_{tot} (28.12, 33.95 wt%), TiO_2 (3.28, 2.27 wt%), Cr (364, 225 ppm) and V (389, 503 ppm), and have compositions referable to Fe-Ti gabbros that suffered oceanic alteration (Gaggero and Gazzotti, 1996). Chloriteschist MJ12 is particularly enriched in Cu (3293 ppm). Talcschists MJ23 and MJ24 are enriched in FeO_{tot} (18.38, 23.62 wt%), TiO_2 (2.5, 1.93 wt%), Cr (199, 385 ppm) and V (306, 316 ppm) even if less than the chloriteschists. They also differ from rhese latter for a peculiar high SiO_2 content (47.15, 38.96 wt%) (Fig. 4b, Table 2). According to Cann (1969), their composition can be typical of gabbro- or basalt-derived breccias cemented by silica. More recently, rocks with similar mineralogy (chloritoid-garnet-talc schists) but different whole rock composition from Pfulwepass (Zermatt Saas zone, Widmer et al., 2000), have been interpreted as derived from hydrothermal veins formed by metasomatism in an ocean floor hydrothermal system.

Hydrothermal alteration of the St. Marcel rocks is supported by oxygen isotope studies performed by Barnicoat and Cartwright (1995). Talcschists from Servette have $\delta^{18}O$ in the range 4.6-5.3‰, glaucophanites in the range 5.2-6.8‰ and mineralised rocks in the range 8.0-8.1‰. Com-

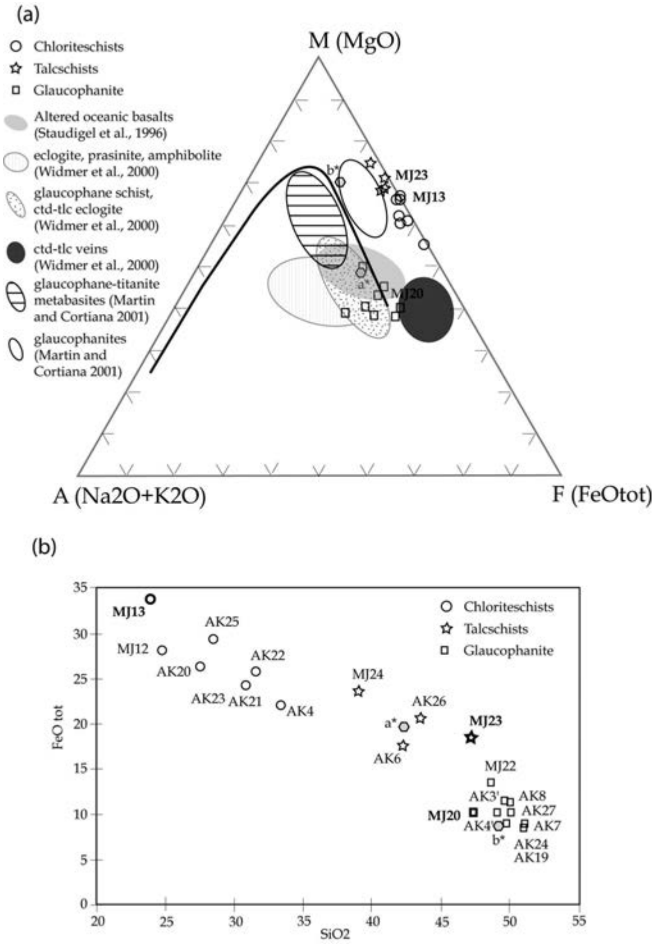

Fig. 4 - Composition of the Servette rocks; circle- chloriteschists; star- talcschists; square- glaucophanite. (a) AFM diagram. The composition of the Piemonte Nappe metabasites from literature is represented by ornamented fields as indicated in the figure. Grey hexagon a* refers to altered oceanic crust (Albarède, 2003); grey hexagon b* refers to unaltered oceanic crust (Engel et al., 1965). (b) Servette rock compositions in the SiO_2 vs FeO_{tot} diagram. Altered (a*) and unaltered (b*) oceanic crust compositions are represented for comparison.

Table 2 - Major (wt%) and trace (ppm) element contents (XRF) of selected rock samples.

	Chloriteschists		Talcschists		Glaucophanite		
Sample	MJ12	MJ13	MJ23	MJ24	MJ20	MJ22	AK7
SiO_2	24,74	23,92	47,15	38,96	47,41	48,63	49,63
TiO_2	3,28	2,27	2,5	1,93	1,7	2,47	1,59
Al_2O_3	19,15	16,9	14,41	16,66	17,53	14,47	17,04
FeO	28,13	33,95	18,39	23,63	10,27	13,40	9,04
MnO	0,27	0,26	0,27	0,37	0,2	0,17	0,16
MgO	11,61	10,58	11,12	10,29	12,05	9,23	11,26
CaO	1,25	1,46	1,66	1,7	2,43	2,65	2,93
Na_2O	0,29	0,48	0,58	0,21	3,08	4,25	3,51
K_2O	0,19	0,23	tr	0,21	0,12	0,18	0,03
P_2O_5	0,45	0,38	0,25	0,25	0,2	1,41	0,23
H_2O	7,91	6,31	2,97	3,33	4,12	1,87	2,9
Total	97,27	96,74	99,30	97,54	99,11	98,73	98,32
Ba	142	149	39	104	66	57	30
Cu	3293	418	565	58	72	78	29
Rb	60	63	54	67	75	72	12
Sr	18	0	81	0	63	43	56
Y	13	38	12	23	27	23	25
Nb	9	8	10	9	10	7	7
Zr	105	185	135	101	93	154	96
Co	169	108	124	68	35	41	37
Cr	364	225	199	385	403	291	381
Ni	29	13	27	26	105	19	113
V	389	503	306	316	234	323	281
Zn	127	44	242	93	80	131	109
S	2534	977					

paring these values with $\delta^{18}O$ data of homogeneous basalts (range: 4-9.5‰) and pillow lavas (range: 7.1-9.1‰) of the Macquarie Island ophiolites that escaped high pressure metamorphism (see Fig. 4 of Cartwright and Barnicoat, 1999), the Servette rocks appear to preserve $\delta^{18}O$ values reflecting a hydrothermal alteration that occurred below the ocean floor. In fact, these values are similar to the value of about 5.7‰ estimated by the authors for the oceanic basalts and gabbros. According to Cartwright and Barnicoat (1999), in the higher levels of the oceanic crust, interaction with sea water at low temperature results in increasing $\delta^{18}O$ values, whereas higher temperature alteration at deeper levels causes $\delta^{18}O$ values to be lowered. The pattern of isotopic resetting is also dependent on whether the rocks are situated in the downflow parts of the hydrothermal system (where temperatures are relatively cool) or in the warmer upflow zones.

The mineralogy of the St. Marcel "blueschists" suggests an enrichment in Mg and H_2O and depletion of very mobile elements such as Ca, Na and Si (see Hajash and Arcker, 1980; Reed, 1983), with formation of chlorite and breakdown of plagioclase, which are typical of basalts from downflow zones.

By contrast, chloritoid-garnet bearing talcschists depleted in silica (e.g., MJ24) probably derive from hydrothermal upflow zones that underwent high-temperature sub-ocean floor alteration, as confirmed by $\delta^{18}O$ values lower than 5.7‰.

The Servette mineralised rocks associated with talcschists and including sulphide, quartz, glaucophane, garnet, cummingtonite, have high $\delta^{18}O$ values and probably represent fossil black-smoker-type deposits (Barnicoat and Botwell, 1995).

Besides the oceanic hydration, the mafic rocks of St. Marcel could have been saturated in H_2O during subduction, by acquiring water released by breakdown of serpentinites deeper in the subduction zone, as proposed by Bucher et al. (2005) for the "blueschists" of the Pfwulve area.

Anhydrous rocks (eclogites and metagabbros) in the Servette slice are scarce; their formation was contemporaneous with that of glaucophanite, talcschists and chloriteschists as indicated by field and microstructural evidence. All these rocks formed together at maximum pressure conditions.

MINERAL CHEMISTRY

Minerals have been analysed using a CAMEBAX microprobe, operating at the Laboratoire de Pétrologie, Université Paris VII. Operating conditions were 20 kV and 20 nA, and various minerals and pure oxides were used as standards. Representative microprobe analyses are reported in Tables 3 to 5.

Garnet

Large garnets are present in all lithologies. Fe^{3+} contents, estimated through stoichiometric calculations, are negligible (Table 3), so that all Fe can be assumed to be Fe^{2+} (i.e. $Fe_{tot} = Fe^{2+}$). Garnets show zonations, as shown in Fig. 5; in chloriteschists and talcschists the Fe content first increases and then decreases from core to rim, while Mg increases and Mn and Ca decrease toward the rim. On the contrary, in glaucophanite Fe and Ca contents are rather constant. X_{Fe} $[Fe^{2+}/(Fe^{2+} + Mg)]$ ratio varies between 0.76 in glaucophan-

Table 3 - Compositions of garnets (g) from chloriteschist MJ13, talcschist MJ23 and glaucophanite MJ20.

Sample	MJ13			MJ23								MJ20	
Analysis	35	55	57	75	79	82	86	89	92	94	97	95(P)	102c
Mineral	g	g	g	g	g	g	g	g	g	g	g	g	g
SiO_2	37,66	36,9	36,81	36,99	36,97	36,93	36,94	36,87	36,91	36,6	37,05	38,17	37,72
TiO_2	0,03	0,17	0,12	0,07	0,1	0,11	0,15	0,1	0,1	0,14	0,1	0,06	0,08
Al_2O_3	20,91	20,64	20,54	20,88	20,69	20,54	20,37	20,35	20,66	20,08	20,79	21,31	21,2
Cr_2O_3	0,01	0,02	0,03	0,09	0,03	0,04	0,04	0,06	0,07	0,02	0,07	0,04	0,03
FeO	34,10	27,36	27,43	37,85	34,21	33,27	31,86	32,76	34,23	35,32	36,76	27,93	27,19
MnO	0,17	4,5	4,43	0	0,19	0,52	1,65	0,62	0,19	0,08	0,05	1,4	4,44
MgO	4,03	1,04	1	2,99	1,45	1,23	1,05	1,19	1,44	1,8	2,33	4,96	3,56
CaO	2,91	8,29	8,12	0,98	5,94	6,89	7,34	7,28	5,93	4,88	2,7	5,98	5,86
Na_2O	0	0,07	0,09	0,03	0,01	0,04	0,08	0	0,05	0	0	0	0,02
K_2O	0	0	0	0	0	0	0	0	0	0	0	0	0
Totals	99,83	99,04	98,61	99,91	99,63	99,65	99,58	99,31	99,65	99,03	99,86	99,87	100,15
Oxygens	12	12	12	12	12	12	12	12	12	12	12	12	12
Si	3,009	2,993	2,999	2,991	2,994	2,99	2,993	2,995	2,989	2,99	2,999	3,002	2,99
Ti	0,002	0,01	0,007	0,004	0,006	0,007	0,009	0,006	0,006	0,009	0,006	0,004	0,005
Al	1,97	1,974	1,973	1,99	1,976	1,96	1,946	1,949	1,973	1,934	1,984	1,976	1,981
Cr	0,001	0,001	0,002	0,006	0,002	0,003	0,003	0,004	0,004	0,001	0,004	0,002	0,002
$Fe3^+$	0,008	0,03	0,027	0,019	0,024	0,05	0,059	0,045	0,04	0,066	0,002	0,01	0,03
$Fe2^+$	2,27	1,826	1,842	2,54	2,294	2,202	2,1	2,181	2,278	2,347	2,486	1,827	1,772
Mn	0,012	0,309	0,306	0	0,013	0,036	0,113	0,043	0,013	0,006	0,003	0,093	0,298
Mg	0,48	0,126	0,121	0,36	0,175	0,148	0,127	0,144	0,174	0,219	0,281	0,581	0,421
Ca	0,249	0,72	0,709	0,085	0,515	0,598	0,637	0,634	0,515	0,428	0,234	0,504	0,498
Na	0	0,011	0,014	0,005	0,002	0,006	0,013	0	0,008	0	0	0	0,003
K	0	0	0	0	0	0	0	0	0	0	0	0	0
Sum	8	8	8	8	8	8	8	8	8	8	8	8	8
X_{Fe}	0,83	0,94	0,94	0,88	0,93	0,94	0,94	0,94	0,93	0,91	0,90	0,76	0,81

Table 4 - Composition of chloritoids from chloriteschist MJ13, talcschist MJ23 and glaucophanite MJ20.

Sample	MJ13			MJ23					MJ20	
Analysis	16	19	22	93	97	144	44	53	20	91
Mineral	ctd	ctd	ctd	ctd	ctd	ctd	ctd	ctd	ctd	ctd
SiO_2	25,26	24,67	24,44	24,43	24,62	23,66	25,15	25,38	25,66	24,38
TiO_2	0	0	0	0	0,11	0,06	0,01	0	0,19	0,05
Al_2O_3	41,03	40,73	40,38	41,24	41,61	40,97	41,57	41,58	42,49	41,14
Cr_2O_3	0	0	0	0,01	0,03	0,01	0,04	0	0,17	0,09
FeO	22,72	22,74	22,11	20,42	19,70	20,60	19,77	20,61	19,44	19,77
MnO	0,05	0,05	0	0	0,14	0,09	0,09	0,02	0,33	0,07
MgO	4,67	5,3	5,51	5,4	5,45	5,15	6,23	6,22	6,16	5,63
CaO	0	0	0	0,05	0,05	0,04	0	0	0	0
Na_2O	0	0,03	0,04	0,03	0,01	0,04	0	0	0,01	0,02
K_2O	0	0	0	0	0	0	0	0	0,09	0
Totals	93,83	93,84	92,8	91,68	91,73	90,82	92,96	93,97	94,56	91,24
Si	1,014	0,99	0,989	0,994	0,999	0,975	1,005	1,006	1,007	0,995
Ti	0	0	0	0	0,003	0,002	0	0	0,006	0,002
Al	1,942	1,926	1,927	1,979	1,991	1,989	1,958	1,943	1,967	1,979
Cr	0	0	0	0	0,001	0	0,001	0	0,005	0,003
$Fe3^+$	0,03	0,097	0,098	0,035	0,004	0,061	0,029	0,045	0,007	0,026
$Fe2^+$	0,733	0,666	0,651	0,66	0,664	0,649	0,631	0,638	0,631	0,648
Mn	0,002	0,002	0	0	0,005	0,003	0,003	0,001	0,011	0,002
Mg	0,28	0,317	0,332	0,328	0,33	0,316	0,371	0,368	0,36	0,342
Ca	0	0	0	0,002	0,002	0,002	0	0	0	0
Na	0	0,002	0,003	0,002	0,001	0,003	0	0	0,001	0,002
K	0	0	0	0	0	0	0	0	0,005	0
X_{Mg}	0,28	0,32	0,34 #	0,33	0,33	0,33	0,37	0,37 #	0,36	0,35
Sum	4	4	4	4	4	4	4	4	4	4

ite and 0.94 in chloriteschists. Garnet composition is affected by whole rock chemistry, with Fe-rich garnets in chloriteschists and Mg-rich garnets in glaucophanite (Fig. 5).

Chloritoid

Chloritoid (Fig. 6a) is either found as small inclusions in garnets or as large porphyroblasts. Chloritoid from chloriteschists is more Fe-rich ($X_{Mg} = 0.27\pm0.07$) than chloritoid from talcschists ($X_{Mg} = 0.33\pm0.07$) and glaucophanite ($X_{Mg} = 0.35\pm0.05$), thus reflecting the whole rock composition (Table 4, Fig. 6a). The Fe^{3+} content, calculated imposing $Al + Fe^{3+} = 4$, is always very low ($X_{Fe^{3+}} < 0.03$). Mn is always absent or very low, except in sample MJ20. Chloritoid included in garnet is Fe-richer than the one in the matrix of the same rock.

Amphibole

Blue amphiboles include glaucophane and "crossite" (Table 5). Crossite is found in chloriteschists, the more Fe-rich rocks (e.g., sample MJ13), while glaucophane is present in talcschists (Fig. 6b). $X_{Ca} = Ca/(Ca + Na)$ is always lower than 0.05 and Na is always higher than 1.5 apfu.

Chlorite

Chlorite (Fig. 6c and Table 5) is mainly between clinochlore and ripidolite in composition, according to Wiewiora and Weiss (1990). Balancing chlorite formulae (charge balance) we derive that no, or very little, Fe^{3+} is present. Compositions have a wide range, with Mg-rich chlorite in glaucophanite ($X_{Mg} > 0.7$) and Fe-richer chlorite in chloriteschists ($X_{Mg} < 0.6$). Moreover, in the same sample, retrogressive chlorite (replacing garnet and chloritoid

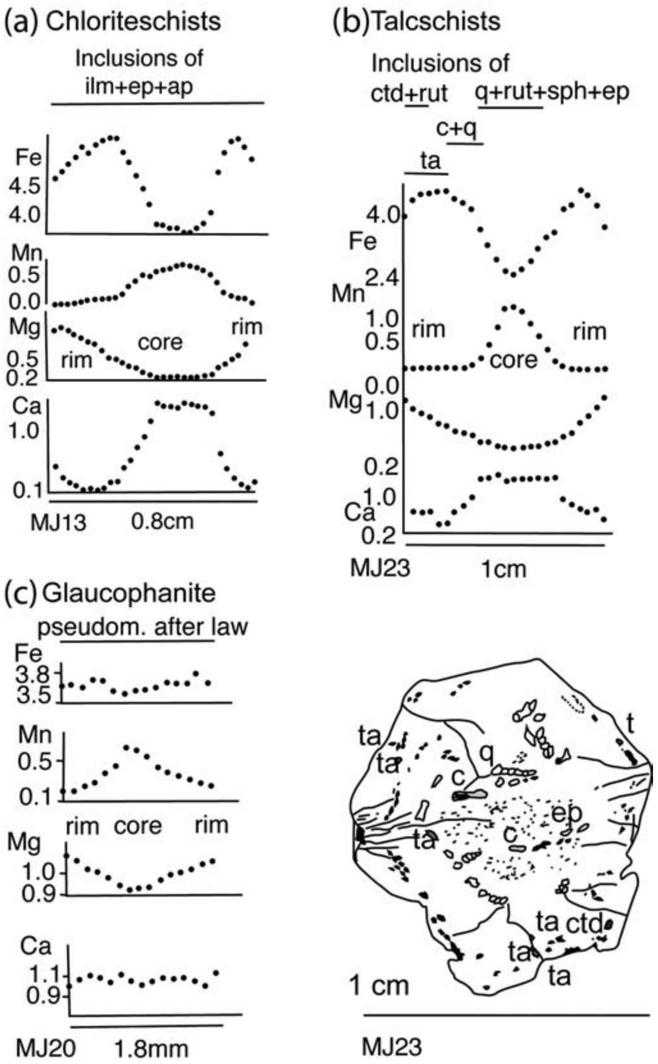

Fig. 5 - Compositional profiles of garnet in representative samples (a- chloriteschists; b- talcschists; c- glaucophanite). Inclusions are indicated in the upper part of each figure, horizontal bars showing their distribution. Symbols as in other figures, except for: c- cummingtonite; ap- apatite; q- quartz; ilm- ilmenite; rut- rutile. Inclusion species and their positions in a garnet from sample MJ23 (talcschist) are drawn in the lower right part of the figure.

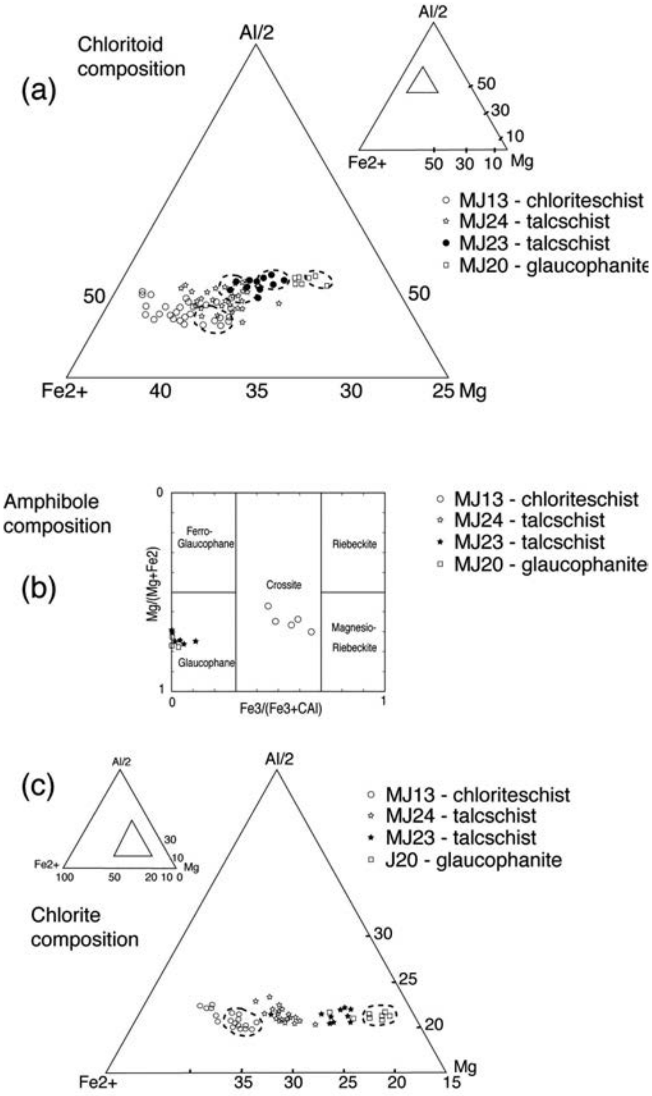

Fig. 6 - (a) Chloritoid composition in Al/2, Fe^{2+}, Mg diagram; (b) amphibole composition in the Miyashiro diagram and (c) chlorite composition in Al/2, Fe^{2+}, Mg diagram. Circled areas enclose points representing chloritoid found as inclusions in garnets and chlorite that coexists with high-pressure minerals, respectively. Points outside this area correspond to secondary chlorite (determined on textural evidences). Sample names as in Fig. 4, description in the text.

Table 5 - Compositions of paragonite (pa), talc (ta), chlorite (chl) and glaucophane (gl) from chloriteschist MJ13, talcschist MJ23 and glaucophanite MJ20.

Sample	MJ13	MJ23							MJ20
Analysis	11	72	60	b	1	2	7	22	27
Mineral	pa	ta	ta	pa	chl	chl	gl	gl	gl
SiO_2	46,8	59,6	60,97	46,89	26,13	25,67	55,87	58,71	59,25
TiO_2	0,07	0,11	0	0	0,04	0,11	0,03	0	0,04
Al_2O_3	38,46	0,18	0,1	39,35	20,85	20,29	6,27	10,69	11,57
Cr_2O_3	0	0,06	0,01	0	0,05	0,04	0,06	0,44	0
FeO	1,23 #	7,13	5,84 #	0,98 #	22,91	25,44	18,22	8,74	6,73
MnO	0,01	0	0	0	0,17	0,15	0,02	0	0,03
MgO	0,1	26,05	27,26	0,34	16,89	15,86	8,8	11,41	12,06
CaO	0,06	0,1	0	0,16	0	0	1,8	0,71	0,37
Na_2O	7,18	0,02	0	7,37	0	0	6,25	7,22	7,35
K_2O	0,91	0	0	0,58	0	0	0	0	0
Totals	94,82	93,29	94,21	95,67	87,06	87,62	97,88	98,04	97,47
Oxygens	11	11	11	11	14	14	23	23	23
Si	3,019	3,978	4	2,992	2,735	2,709	7,962	7,973	7,996
Ti	0,003	0,006	0	0	0,003	0,009	0,003	0	0,004
Al	2,925	0,014	0,008	2,96	2,573	2,524	1,053	1,711	1,841
Cr	0	0,003	0,001	0	0,004	0,003	0,007	0,047	0
$Fe3^{+}$	0	0,018	0	0	0	0,036	0,593	0,118	0,068
$Fe2^{+}$	0,066	0,38	0,32	0,052	2,006	2,21	1,578	0,874	0,692
Mn	0,001	0	0	0	0,015	0,013	0,002	0	0,003
Mg	0,01	2,591	2,668	0,032	2,637	2,497	1,869	2,309	2,426
Ca	0,004	0,007	0	0,011	0	0	0,275	0,103	0,054
Na	0,898	0,003	0	0,912	0	0	1,729	1,903	1,925
K	0,075	0	0	0,047	0	0	0	0	0
Sum	7,001	7	6,996	7,007	9,973	10,001	15,072	15,04	15,008

along fractures) is always Fe- and Al-richer and Si-poorer than the chlorite coexisting with high pressure minerals (*e.g.* $X_{Mg}^{Chl-HP} = 0.76$ and $X_{Mg}^{Chl-retr} = 0.70$ in chloriteschist MJ13).

Talc

Talc (Table 5) has a homogeneous composition with $X_{Mg} = 0.87$-0.89, except in sample MJ20, where it shows $X_{Mg} = 0.90$-0.91. Talc included in chloritoid or garnet has X_{Mg} (from 0.79 to 0.86) always lower than the talc found in the matrix of the same sample. Sometimes small amounts of Mn and Al^{3+} are present. Talc is stable together with glaucophane, chloritoid and garnet at peak P-T conditions and survives in the retrograde assemblages until chloritoid disappears, but there is no compositional change in talc occurring in different microtextures.

P-T ESTIMATES

Summary of microtextural observations - general remarks

According to textural evidence the metamorphic evolution of the Servette rocks can be summarised as follows:

– the prograde path is indicated by pseudomorphs after lawsonite (now zoisite/clinozoisite + paragonite ± albite ± calcite ± chlorite) in glaucophanite and by minerals included in garnet cores of the glaucophanite (garnet, chlorite, glaucophane, pseudomorphs after lawsonite, paragonite and chloritoid). Omphacite has never been observed as inclusion in garnets;

– the pervasive foliation in the glaucophanite corresponds to S_2 and it is characterised by the equilibrium assemblage garnet, chlorite, glaucophane, paragonite and talc. Absence of jadeite and kyanite, and presence of prograde paragonite suggests P < 2.5 GPa (see Guiraud et al., 1990). Presence of chlorite limits T below 650°C, while coexistence of glaucophane, chloritoid, garnet, chlorite and paragonite implies P > 1.8 GPa (Guiraud et al., 1990);

– greenschist-facies retrogression is indicated by the following observations: in chloriteschists garnet is overgrown by chlorite and quartz along rims and cracks, and chloritoid and glaucophane are transformed to paragonite + chlorite. In glaucophanite and talcschists, garnet is replaced by chlorite, chloritoid and glaucophane is overgrown by chlorite + paragonite + quartz.

Estimated peak P-T conditions

Estimated P-T conditions of the peak assemblages have been inferred following two methods: i) direct P-T calculation using mineral compositions and THERMOCALC 3.2 average PT calculation mode; ii) by modelling and calculating P-T pseudosections for compositions representing the three main lithologies at the peak conditions and using again the program THERMOCALC 3.25 and the related internally consistent thermodynamic database (Holland and Powell, 1998).

Table 6 - Modal composition of representative samples and calculated bulk rock compositions used in pseudosections (in mole %).

	Chloriteschist	Talcschist	Glaucophanite
	MJ13	MJ23	MJ20
g	25	36	11
chl	62,5	8	17,2
ctd	1,5	2	12
gl	0,1	4,2	44,4
cz	1	0,1	7
ta	0,1	18	8,5
pa	1,5	0,1	8
q	0,1	28,2	2
x(ctd)	0,72	0,68	0,61
x(chl)	0,155	0,13	0,12
y(chl)	0,63	0,665	0,65
x(ta)	0,13	0,11	0,1
y(ta)	0,005	0,005	0,005
z(pa)	0,1	0,011	0,015
x(g)	0,8	0,79	0,63
z(g)	0,06	0,08	0,17
x(gl)	0,48	0,29	0,26
n(gl)	0,97	0,97	0,97

	SiO_2	Al_2O_3	CaO	MgO	FeO	Na_2O
chloriteschist	37,73	16,08	1,17	35,91	8,94	0,16
talcschist	53,98	14,64	2,57	22,17	2,37	4,25
glaucophanite	64,67	8,04	1,42	15,2	10,33	0,34

x(mineral) = Fe/(Fe+Mg), y(chl) = Al/4, y(ta) = xAl4, z(pa) = Ca/(Ca+Na), z(g) = Ca/(Fe+Mg+Ca), n(gl) = Na/(Na+Ca).

Geothermobarometry

The stability conditions for the mineral compositions of the assemblages observed in chloriteschists, talcschists and glaucophanite have been determined. Our calculations gave relatively homogeneous values for the high-pressure re-equilibration, with temperatures of 550 ± 60° and pressures of 1.9 ± 0.4 GPa.

Modelling the equilibrium assemblages

Three P-T pseudosections (Fig. 7) have been calculated for compositions representative of samples MJ13 (chloriteschist), MJ23 (talcschist) and MJ20 (glaucophanite) using the dataset and the activity-composition relationships of minerals used by Wei et al. (2003) and Dale et al. (2005). Analysed bulk rock compositions (Table 2) cannot be used to calculate the pseudosections because all the samples contain zoned minerals: for example garnet cores and the included relict minerals represent subdomains not in equilibrium with the matrix minerals. This means that in order to be

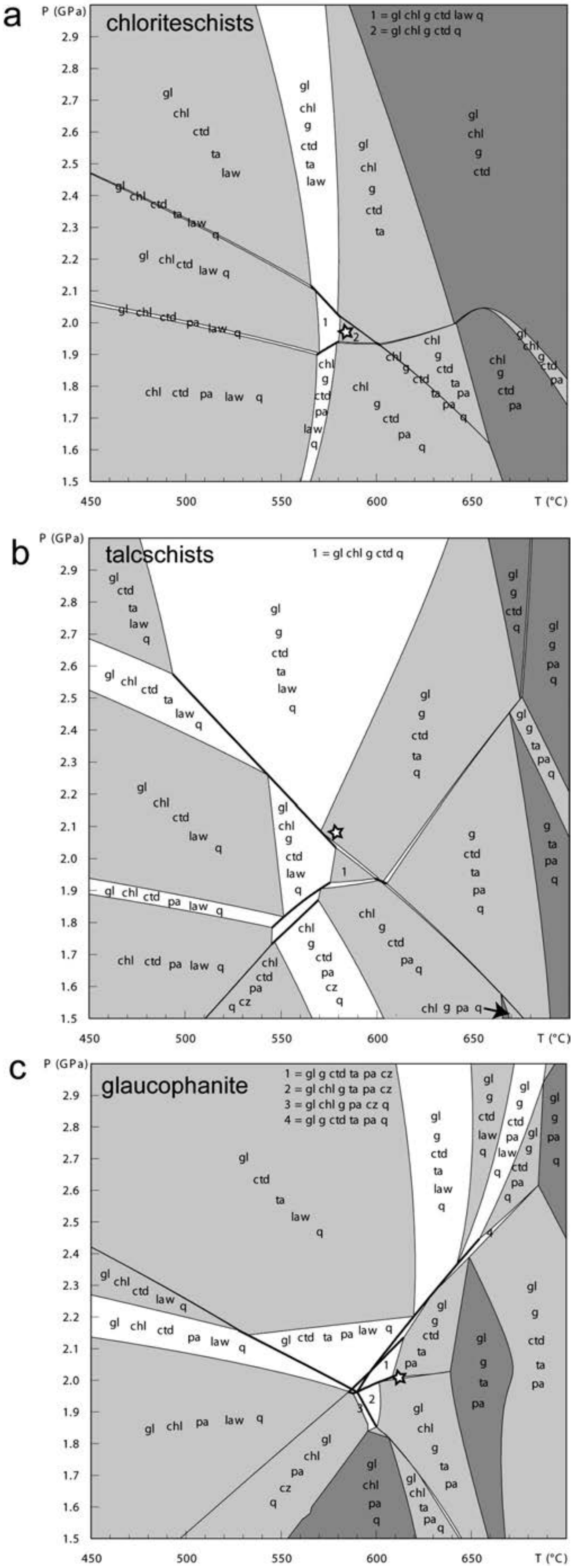

Fig. 7 - P-T pseudosections calculated for the main lithologies: (a) chloriteschists, (b) talcschists and (c) glaucophanite. A star indicates the field with the observed peak high-pressure equilibrium assemblage. The bulk composition is expressed on the basis of the normalised mole proportions of the NCFMASH as: (a) SiO_2 = 36.63, Al_2O_3 = 15.61, CaO = 1.14, MgO = 34.87, FeO = 11.59, Na_2O = 0.16 (chloriteschist MJ13); (b) SiO_2 = 54.26, Al_2O_3 = 11.48, CaO = 2.02, MgO = 21.70, FeO = 10.05, Na_2O = 0.48 (talcschist MJ23); (c) SiO_2 = 54.41, Al_2O_3 = 13.73, CaO = 2.41, MgO = 20.80, FeO = 4.66, Na_2O = 3.99 (glaucophanite MJ20). Univariant reactions calculated for various compositions are shown as thicker lines, divariant fields are unornamented six-phase areas, trivariant fields are light coloured five-phase areas, and quadrivariant fields are dark-coloured four-phase areas.

able to determine the actual composition that was reacting during the formation of syn-S_2 peak mineral assemblages, we have to disregard from the analysed bulk composition the components already fractionated in the garnet cores. We have therefore considered the average modal composition of matrix minerals of each sample which represents the equilibrium assemblage at peak high-pressure conditions (as inferred from microstructural and textural observations, Fig. 3 and Table 6).

The final compositions used to calculate the pseudosections are summarised in Table 6 (see calculated molar compositions at the bottom of the Table). Fe^{3+} has not been considered in our model for several reasons: we have not measured it, but the high-pressure minerals seem to have little Fe^{3+} as deduced from charge balance considerations in cation calculation. Moreover, we do not have good activity models to account for it in all our minerals.

Omphacite has not been used to calculate our pseudosections because we have never observed it in any of the studied samples. Omphacite-garnet classic eclogites are present in the area, but they are few and far from the Servette mine. We have however checked through some preliminary calculations (supported by results obtained by Bucher on glaucophanites, personal communication) where omphacite would have been stable in our pseudosections. Results show that omphacite would be stable in our rocks at pressures higher than those at which the observed assemblages are stable. The fact that we have never observed even a single omphacite grain in the matrix or as inclusion in garnet would suggest that omphacite was never stable in our “blueschist” rocks, differently to what observed by Bucher et al. (2005) in rocks from the Pfulwe region in the Zermatt-Saas Unit.

The three pseudosections (Fig. 7) reflect differences in composition of the rocks and the different parageneses at equilibrium. These pseudosections are characterised by univariant reactions and divariant, trivariant and quadrivariant fields. Lawsonite is always limited to low temperature (see also Rebay and Powell, 2002 and Wei et al., 2003). The reaction

$$\text{law} = \text{ky} + \text{zo} + \text{q} + H_2O$$

defines the thermal limit of lawsonite stability in the CASH system. For the glaucophanite composition, the stability field of lawsonite is somewhat wider than that for chloriteschist and talcschist compositions, where it is limited at T < 500-600°C (Fig. 7). This could explain the pseudomorphs after lawsonite found only in the glaucophanite. Nonetheless, no lawsonite relic has been found so far (only pseudomorphs) thus implying that all lawsonite has been consumed during the prograde or retrograde evolution.

In Fig. 7 garnet is stable at slightly higher temperatures in glaucophanite than in chloriteschist and talcschist. This is due to the peculiar Mg-rich calculated compositions of these rocks (deriving from the Mg-rich composition of the garnet rims at equilibrium with the matrix minerals used to calculate the pseudosections), and also to the fact that Mn has not been considered in the model system: its presence (see Table 3) results in lowering the stability temperature of garnet-bearing assemblages. The pseudosections are calculated for compositions reflecting only the peak assemblages and should not be used as regards to the whole metamorphic evolution.

Fig. 7a (chloriteschist MJ13) is characterised by trivariant and quadrivariant fields. One invariant point (i2, Table 7) and 5 invariant lines (u2, [law, cz], u3, [law, ta], u9, [cz, ta], u11, [pa, ta] and [gl, ta], u15 [pa, cz]) are calculated for this composition. Divariant fields are very narrow. The assemblage garnet, chlorite, glaucophane, chloritoid, talc, quartz is limited to a divariant field around 2.0 GPa and 590°C. Paragonite is stable at slightly lower temperatures and pressures. The fact that paragonite is stable at pressure well above its stability in the CNASH subsystem is partly due to compositional differences of the entire system. Chlorite and chloritoid are always stable, so that chlorite is effectively in equilibrium with the different assemblages during the entire evolution, even above 550°C. Its composition changes, being Mg-richer at higher pressures.

Table 7 - Invariant points and univariant reactions of Figure 8.

Invariants		P (GPa)	T (°C)
i1	[law]	1,88	611
i2	[ta]	1,88	569,3
i3	[pa]	1,99	588,4
i4	[g]	1,94	582,2

Univariants		reaction
u1	[law, q]	g pa chl ta = gl ctd cz H2O
u2	[law, cz]	g pa chl q = gl ctd ta H2O
u3	[law, ta]	g pa chl q = gl ctd cz H2O
u4	[law, ctd]	chl gl cz q = g pa ta H2O
u5	[law, gl-pa]	chl cz q = g ctd ta H2O
u6	[law, chl]	gl ctd cz q = g pa ta H2O
u7	[law, g]	pa chl cz q = gl ctd ta H2O
u8	[ta, q]	g pa chl law = gl ctd cz H2O
u9	[ta, cz]	g pa chl q = gl ctd law H2O
u10	[ta, ctd]	g gl law = pa chl cz q H2O
u11	[ta, gl-pa]	g chl law = ctd cz q H2O
u12	[ta, chl]	g gl law = pa ctd cz q H2O
u13	[ta, g]	gl ctd law = pa chl cz q H2O
u14	[pa, q]	g chl law = ctd ta cz H2O
u15	[pa, cz]	chl law q = g ctd ta H2O
u16	[pa, ctd]	g ta law = chl cz q H2O
u17	[pa, chl]	g ta law = ctd cz q H2O
u18	[pa, g]	chl law q = ctd ta cz H2O
u19	[g, q]	chl gl law = pa ctd ta cz H2O
u20	[g, cz]	pa chl law q = gl ctd ta H2O
u21	[g, ctd]	gl law = pa chl ta cz q H2O
u22	[g, chl]	gl law = pa ctd ta cz q H2O

Fig 7b (talcschist MJ23) is dominated by tri- and quadrivariant fields on the high temperatures side, and by divariant fields at lower temperatures (and higher pressures). No invariant points are seen, and the four univariant reactions u9 [ta, cz], u11 [ta, n], u15 [pa, cz] and u20 [law, cz] (Table 7) are calculated for this composition. The high-pressure equilibrium assemblage garnet, glaucophane, chloritoid, talc, quartz is stable in a trivariant field extending from 1.9 GPa up and from 570 to 660°C. Addition of chlorite would restrict it to a narrow divariant field from 1.9 to 2.1 GPa and 570-610°C (Fig. 7).

In both pseudosections (Fig. 7a and b) it is possible to observe that the presence of lawsonite would be restricted to prograde conditions, and that during retrograde evolution talc would be consumed before chloritoid. Chloritoid is stable at temperatures < 700°C, and in fact we find it as inclusions in garnets (prograde path), as part of the higher pressure assemblages, and only partially altered (chlorite rims) during the retrograde path. Talc is stable in the entire diagram, except for higher temperatures. Paragonite is stable for pressures < 2.1 GPa (and it is often, on textural ground, a retrograde mineral).

Fig. 7c (glaucophanite MJ20) is dominated by trivariant fields, with few divariant and quadrivariant fields. Two invariant points (i1 and i4), and 9 univariant reactions (u1, [law, q], u4, [law, ctd], u6, [law, chl], u7, [law, g], u12, [ta, chl], u13, [ta, g], u17, [pa, chl], u20, [g, cz] and u22, [g, chl], Table 6) are calculated for this composition. The high-pressure equilibrium assemblage (gl + ctd + g + chl + pa ± ta) is observed for pressures between 2 and 2.1 GPa but for slightly higher temperatures than the other rocks, between 600° and 650° C.

Glaucophane (gl) is always stable, whereas chloritoid is stable for pressures > 1.9 GPa. Garnet is stable only at temperatures > 590°C, which is not in perfect agreement with all other observations that indicate that the Servette rocks were stable for temperatures below 600°C along their whole evolution. This is an effect of the composition assumed for glaucophanites, which is problematic as they have many large zoned garnet and chloritoid porphyroclasts with different inclusions that should be excluded from the composition reacting during formation of the D_2 assemblage.

DISCUSSION

Peak PT conditions

The present peak estimates T = 550 ± 60°C and P = 2.1 + 0.3 GPa of the Servette rocks are higher than those (T = 550 ± 20°C and P= 1.2 ± 0.1 GPa) obtained via traditional thermobarometry in glaucophanites and eclogites by Tartarotti, (1988) and Martin and Tartarotti (1989). These estimates were in the same range of those calculated by Brown et al (1978), Mottana (1986) and Martin and Kienast (1987) for the eclogite Mn-assemblages in Praborna (Tmax = 500°C and P max = 1.4 GPa). All these P-T values had been estimated to be consistent with the metamorphic conditions of the St. Marcel eclogites, characterized by absence of kyanite and Mg-chloritoid. However, these estimates are thought to reflect the state of the art in thermobarometry at the time of the publications. Similarly, estimations of the P-T conditions in different places of the Zermatt Saas Unit via traditional thermobarometry utilizing exchange and net-transfer equilibria pertinent to the assemblages observed in the rocks of Allalin (Bearth, 1967; Barnicoat and Fry, 1986), Cignana (Reinecke, 1982) and Taschalp-Pfulwe (Widmer et al., 2000) gave a large P-T range spanning from 450-700°C and 1.0-2.5 GPa. (e.g., for Allalin rocks: 500-700°C and 1.0-1.5 GPa, Chinner and Dixon, 1973; 550-600°C and 1.7-2.0 GPa, Barnicoat and Fry, 1986; 650°C and 2.5 GPa, Bucher and Frey, 1994; for Taschalp-Pfulwe rocks: 550-575°C and 1.8-2.4 GPa, Ganguin, 1988; 550-600°C and 1.7-2.0 GPa, Barnicoat and Fry, 1986; for Breuil-St. Jacques, T = 470±50°C and P = 1.0±0.2 GPa, Ernst and Dal Piaz, 1978). To resolve these P-T inconsistencies for the Zermatt-Saas zone, recently Bucher et al. (2005) carried out a new evaluation of the peak P-T conditions, calculating stability assemblages under excess water for the Pfulwe eclogites and glaucophanites. These authors obtained conditions of 2.7-2.8 GPa at 580°C, which coincide with those obtained by Reinecke (1991; 1998) and van der Klauw et al. (1997) from coesite-bearing quartzite associated with metabasite at Lago di Cignana. Because no regional mineral zone boundaries or isogrades have been identified in the Zermatt-Saas zone until now, according to Bucher et al. (2005), these rocks may have experienced the same peak P-T conditions (P = 2.8 ± 2 GPa and T = 550-600°C), and have been detached together, at the same time and by the same mechanism from the subducting Tethys lithosphere to be exhumed. It is not possible, however, with the data available from the whole Zermatt-Saas zone, to exclude that other parts of this zone, which extends over several hundreds of kilometres, experienced different P-T evolution and P-peak conditions. This could explain the different pressure peak conditions that we obtained in the studied area, which lies South of the Ranzola fault (Fig. 1).

CONCLUSIONS

The mineralogy of the St. Marcel "blueschists", and in particular of the Servette slice, strongly depends on the pre-Alpine pervasive hydrotermal alteration that occurred either below the Mesozoic seafloor, as confirmed by $\delta^{18}O$ isotope values (< 6) and sulphide mineralisations, or at the seafloor as suggested by increasing $\delta^{18}O$ isotope values (> 6 in some blueschists) and Mn mineralisations.

The prograde subduction path is constrained by widespread occurrence of lawsonite pseudomorphs and glaucophane in glaucophanites, either in garnet cores or in the matrix; by quartz, titanite, chloritoid in garnet cores in chloriteschists; by quartz, titanite, cummingtonite and crossite included in the garnet cores of talcschists.

P-T peak minerals of the glaucophanite are glaucophane, garnet, chloritoid, epidote, paragonite, talc, phengite, rutile, sulphide, without quartz and omphacite; peak minerals of the chloriteschists are chlorite, chloritoid, garnet, sodic amphibole (crossite), rutile, sulphide, ilmenite and allanite; and those of talcschists are talc, chloritoid, garnet, rutile, sulphide and glaucophane.

P-T calculation by means of classical geothermobarometry and equilibrium assemblage stability for specific bulk compositions, allows to define peak conditions of T = 550 ± 60°C and P = 2.1 ± 0.3 Gpa.

These values are higher than those proposed previously for the Servette rocks and lower than those calculated for the Zermatt-Saas metaophiolites north of the Ranzola fault. No coesite has been found so far in Servette, even though mineral assemblages of mafic compositions are similar to those found is rocks north of the Ranzola fault and quartz-bearing rocks are abundant. Nonetheless, no omphacite has been observed in the garnet core of the glaucophanite.

The Servette mafic rocks, already hydrated by hydrothermal alteration, were located in the Tethys descending slab and became saturated in H_2O by acquiring the water released by associated serpentinites (Mt. Avic?), deeper in the subduction zone. However, they escaped a further pervasive late metamorphic re-equilibration which, instead, mainly concentrated along the regional-scale shear zones beneath the Mt. Emilius.

The peculiar mineralogy of the Servette rocks is thus due to the special composition of the protoliths and to their structural relationships. These factors favoured the development of the hydrous high-pressure (P = 2.1±0.3 Gpa) mineral assemblages described in this paper.

ACKNOWLEDGMENTS

A first draft of this manuscript was improved thanks to the comments of T. Hirajima, H.K. Ravna, K. Bucher and one anonymous reviewer. The authors are thankful to Mike

Brown and Roger Powell for comments, English revision and petrological help. An anonymous reviewer and Paola Tartarotti allowed a further improvement of the present manuscript.

With this paper, we would like to thank Jean Robert Kienast (one of the authors) for introducing Silvana Martin to the petrology of the St. Marcel rocks and Gisella Rebay to the “pseudosection mistery” during their PhD and post-doc in Paris, respectively.

REFERENCES

Alt J.C. and Honnorez J., 1984. Alteration of the upper oceanic crust, DSDP site 417: mineralogy and chemistry. Contrib. Mineral. Petrol., 87: 149-169.

Alt J.C., Honnorez J., Laverne S. and R. Emmerman, 1986. Hydrothermal alteration of a 1 km section through the upper oceanic crust, DSDP Hole 504B: mineralogy, chemistry, and evolution of sea-water-basalt interactions. J. Geophys. Res., 91: 10309-10335.

Barnicoat A.C. and Bowtell S.A., 1995. Seafloor hydrothermal alteration in metabasites from high-pressure ophiolites of the Zermatt-Aosta area of the western Alps. Boll. Mus. Sci. Nat. Torino, 13 (Suppl.): 191-220.

Barnicoat A.C. and Cartwright I., 1995. Focused fluid flow during subduction: oxygen isotope data from high-pressure ophiolites of the western Alps. Earth Planet. Sci. Lett., 132: 53-61.

Barnicoat A.C. and Fry N., 1986. High-pressure metamorphism of the Zermatt-Saas ophiolite zone, Switzerland. J. Geol. Soc. London, 143: 607-618.

Bearth P., 1967. Die ophiolith der Zone von Zermatt-Saas Fee. Beitr. Geol. Karte Schweitz, N.F., 132.

Beccaluva L., Dal Piaz G.V. and Macciotta G., 1984. Transitional to normal MORB affinities in ophiolitic metabasites from the Zermatt-Saas, Combin and Antrona units, Western Alps: implications for the paleogeographic evolution of the western Tethyan basin. Geol. Mijnb., 63: 165-177.

Bernoulli D., Manatschal G., Desmurs L. and Müntener O., 2003. Where did Gustav Steinmann see the trinity? Back to the roots of an Alpine ophiolite concept. Geol. Soc. Am., Spec. Paper, 373: 93-110.

Bocchio R., Benciolini L., Martin S. and Tartarotti P., 2000. Geochemistry of eclogitised Fe-Ti-gabbros from various lithological setting (Aosta Valley, ophiolites, Italian western Alps). Protolith composition and eclogitic paragenesis. Per. Mineral., 69: 217-237.

Bonatti E., Zerbi M., Kay R. and Rydell H., 1976. Metalliferous deposits from the Apennine ophiolites: Mesozoic equivalents of modern deposits from ocean spreading centers. Geol. Soc. Am. Bull., 87: 83-94.

Brongniart A., 1813. Essai d’une classification minéralogique des roches mélangées. Paris, J. Mines, 199: 5-48.

Brown B.P., Essene E.J. and Peacor D.R., 1978. The mineralogy and petrology of Mn-rich rocks from St. Marcel, Piedmont, Italy. Contrib. Mineral. Petrol., 67: 227-232.

Bucher K. and Frey M., 1994. Petrogenesis of metamorphic rocks. 6th Ed. Springer-Verlag, Berlin, 318 pp.

Bucher K., Fazis Y., De Capitani C. and Grapes R., 2005. Blueschists, eclogites, and decompressional assemblages of the Zermatt-Saas ophiolites: high-pressure metamorphism of subducted Tethys lithosphere. Am. Mineral., 90: 821-835.

Cann H.R., 1969. Rb, Sr, Y, Zr and Nb in some oceanic floor basaltic rocks. Earth Planet. Sci. Lett., 10: 7-11.

Cartwright I. and Barnicoat A.C., 1999. Stable isotope geochemistry of Alpine ophiolites: a window to ocean-floor hydrothermal alteration and constraints on fluid-rock interaction during high-pressure metamorphism. Intern. J. Earth Sci., 88: 219-235.

Castello P., 1981. Inventario delle mineralizzazioni a magnetite, ferro-rame e manganese del complesso piemontese dei calcescisti con pietre verdi in valle d’Aosta. Ofioliti: 6, 5-46.

Castello P., Dal Piaz G.V., Gosso G., Kienast J.R., Martin S., Natale P., Nervo R., Polino R. and Venturelli G., 1980. Western Alps ophiolites; The Piemonte ophiolite nappe in the Aosta Valley and related ore deposits. VIth Ophiolite field conf., Italy, Field excursion guidebook, GLOM, Firenze, p. 171-192.

Cesti G., 1978. Il giacimento piritoso-cuprifero di Chuc-Servette presso St. Marcel (Aosta). Rev. Valdôtaine Hist. Nat., 32: 127-156.

Chinner G.A. and Dixon J.E., 1973. Some high-pressure parageneses of the Allalin gabbro, Valais, Switzerland. J. Petrol., 14: 185-202.

Cortesogno L., Lucchetti G. and Penco A.M., 1979. Le mineralizzazioni a manganese nei diaspri delle ofioliti liguri: mineralogia e genesi. Rend. Mineral. Petrol., 35: 151-197.

Dale J., Powell R., White R.W., Elme, F. and Holland T.J.B., 2005. A thermo-dynamic model for Ca-Na clinoamphiboles in Na_2O-CaO-FeO-MgO-Al_2O_3-SiO_2-H_2O for petrological calculations. J. Metam. Geol., 23: 771-791.

Dal Piaz G.V., 1999. The Austroalpine-Piedmont nappe stack and the puzzle of Alpine Tethys. Mem. Sci. Geol., Padova, 51: 155-176.

Dal Piaz G.V. and Ernst W.G., 1978. Areal geology and petrology of eclogites and associated metabasites of the Piemonte ophiolite nappe, Breuil-St Jacques area, Italian Western Alps. Tectonophysics, 51: 99-126.

Dal Piaz G.V. and Omenetto P., 1978. Brevi note su alcune mineralizzazioni della Falda Piemontese in Valle d’Aosta. Ofioliti, 3: 161-176.

Dal Piaz G.V., Cortiana G., Del Moro A., Martin S., Pennacchioni C. and Tartarotti P., 2001. Tertiary age and paleostructural inferences of the eclogitic imprint in the austroalpine outliers and Zermatt-Saas ophiolite, Western Alps. Intern. J. Earth Sci., 90: 668-684.

Dal Piaz G.V., Venturelli G., Spadea P. and Di Battistini G., 1981. Geochemical features of metabasalts and metagabbros from the Piemonte ophiolite nappe, Italian Western Alps. N. Jahrb. Mineral. Abhandl., 142: 248-269.

Debenedetti A., 1965. Il complesso radiolariti-giacimenti di manganese-giacimenti piritoso-cupriferi-rocce a fuchsite, come rappresentante del Malm nella Formazione dei calcescisti. Osservazioni nelle Alpi Piemontesi e della Valle d’Aosta. Boll. Soc. Geol. It., 84: 131-163.

Engel A.E.J., Engel C.G. and Havens R.G., 1965. Chemical charachteristics of oceanic basalts and the upper mantle. Geol. Soc. Am. Bull., 76: 719-734.

Ernst W.G. and Dal Piaz G.V., 1978. Mineral parageneses of eclogitic rocks and related mafic schists of the Piemonte ophiolite nappe, Breuil-St.Jacques area, Italian western Alps. Am. Mineral., 63: 621-640.

Gaggero L. and Gazzotti M., 1996.Primary and secondary oxides, sulfides and accessory minerals in Mid-Atlantic gabbros: mineralogy and petrology. Ofioliti, 21: 105-116.

Ganguin J., 1988. Contribution à la charactérisation du métamorphisme polyphase de la zone de Zermatt-Saas Fee (Alpes Valaisannes). Thèse ETH, Zurich, 8731, 312 pp.

Gass I.G., 1968. Is the Troodos Massif of Cyprus a fragment of Mesozoic ocean floor? Nature, 220: 39-42.

GLOM, 1977. Escursione ad alcuni giacimenti a Cu-Fe e Mn della Falda piemontese, Alpi occidentali: 10-13 ottobre 1977. Ofioliti, 2: 241-263.

Griffin W.L. and Mottana A., 1982. Crystal chemistry of clinopyroxenes from St. Marcel manganese deposit, Val d’Aosta, Italy. Am. Mineral., 67: 568-586.

Guiraud M., Powell R. and Holland T., 1990. Calculated mineral equilibria in the greenschists - blueschists - eclogite facies in Na_2O-FeO-MgO-Al_2O_3-SiO_2-H_2O: methods, results and geological applications. Contrib. Mineral. Petrol., 104: 85-98.

Hajash A. and Archer P., 1980. Experimental seawater/basalt interactions; effects of cooling. Contrib. Mineral. Petrol., 75: 1-13.

Holland T.J.B. and Powell R., 1998. An internally consistent thermodynamic data set for phases of petrological interest. J. Metam. Geol., 16: 309-343.

Honnorez J.J., Alt J.C. and Humphris S., 1998. Vivisection and autopsy of active and fossil hydrothermal alterations of basalt beneath and within the TAG hydrothermal mound. In: P.M. Herzig, S.E. Humphris, D.J. Miller and R.A. Zierenberg (Eds.), Proceed. ODP, Sci. Res., 158: 231-254.

Jervis G., 1873. I tesori sotterranei dell'Italia. Parte prima, regione delle Alpi. Ristampa 1974, Gribaudi Editore, Torino, p. 81-114.

Kienast J.R. and Martin S., 1983. I pirosseni egirin-giadeitici del livello basale di Praborna, Alpi Occidentali. Ofioliti, 8: 245-260.

Knott R., Fouquet Y., Honnorez J., Petersen S. and Bohn M., 1998. Petrology of hydrothermal mineralisation: a vertical section through the TAG mound. In P.M. Herzig, S.E. Humphris, D.J. Miller and R.A. Zierenberg (Eds.), Proceed. ODP, Sci. Res., 158: 5-26.

Krutow-Mozgawa A., 1988. Métamorphisme dans les sédiments riches en fer ou magnesium de la couverture des ophiolites piémontaises (mine de Servette, Val d'Aoste). Thèse Doct., Univ. P.and M. Curie, Paris VI, 166 pp.

Lagabrielle Y. and Cotten J., 1984. Le matériel détritique ophiolitique des séries océaniques liguro-piémontaises. L'example du Haut Queyras. Contribution à l'étude des prasinites. Ofioliti, 9: 43-66.

Lowell R.P., Rona P.A. and von Herzen R.P, 1995. Seafloor hydrothermal system. J. Geophys. Res., 100 (B1): 327-352.

Martin-Vernizzi S., 1982. La mine de Praborna (Val d'Aosta, Italie): une série manganésifère métamorphisée dans la faciès éclogite. Thèse 3rd cycle, Univ. P. and M. Curie, Paris VI, 320 pp.

Martin S. and Cortiana G., 2001. Influence of the whole-rock composition on the crystallization of sodic amphiboles (Piemonte zone, Western Alps. Ofioliti, 26 (2b): 445-456.

Martin S. and Kienast J.R., 1987. The HP-LT manganesiferous quarzites of Praborna, Piemonte ophiolite nappe, Italian Western Alps. Schweiz. Mineral. Petrogr. Mitt., 67: 339-360.

Martin S. and Tartarotti P., 1989. Polyphase HP metamorphism in the ophiolitic glaucophanites of the lower St. Marcel Valley (Aosta, Italy). Ofioliti, 14 (3): 135-156.

Martin S., Godard G. and Rebay G., 2004. The subducted Tethys in the Aosta Valley (Italian Western Alps). 32nd Intern. Geol. Congr., Florence 2004. Field trip Guide book-B02, 48 pp.

Martin S., Tartarotti P. and Dal Piaz G.V., 1994. The Mesozoic ophiolites of the Alps: a review. Boll. Geof. Teor. Appl., 36: 175-219.

Miller J.A. and Cartwright I., 2000. Distinguishing between seafloor alteration and fluid flow during subduction using stable isotope geochemistry: examples from Tethyan ophiolites in the Western Alps. J. Metam. Geol.,18: 467-482.

Moretti A., 1948. Notizie sui giacimenti cupriferi della Valle d'Aosta. Atti Congr. Mineral. It., 237-254.

Mottana A., 1986. Blueschist-facies metamorphism of manganiferous cherts: a review of the Alpine occurrences. Geol. Soc. Am. Bull., 164: 267-299.

Nakamura K., Kato Y., Tamaki K. and Ishii T., 2007. Geochemistry of hydrothermally altered basaltic rocks from the Southwest Indian Ridge near the Rodrigues Triple Junction. Mar. Geol., 239: 125-141.

Natale P., 1966. Osservazioni sul metamorfismo dei minerali metallici nel giacimento piritoso-cuprifero di St. Marcel (Valle d'Aosta). Atti Simp. Intern. Giacimenti Miner. Alpi, Trento, p. 901-904.

Natale P., 1969. Recrystallization and remobilisation in some pyrite deposits of the Western Alps. In: Convegno sulla rimobilizzazione dei minerali metallici e non metallici, Cagliari, 23 pp.

Perseil E.A., 1988. La présence de strontium dans les oxydes manganésifères du gisement de St. Marcel-Praborna (Val d'Aoste, Italie). Mineral. Dep., 23: 306-308.

Perseil E.A. and Smith D.C., 1995. Sb-rich titanite in the manganese concentrations at St. Marcel-Praborna, Aosta Valley, Italy: petrography and crystal chemistry. Mineral. Mag., 59: 717-724.

Pfeifer H.R., Colombi A. and Ganguin J., 1989. Zermatt-Saas and Antrona zone: a petrographic and geochemical comparison of polyphase metamorphic ophiolites of the western-central Alps. Schweiz. Mineral. Petrogr. Mitt., 69: 217-223.

Pineau F., Javoy M., Hawkins J.W. and Craig H., 1976. Oxygen isotope variations in marginal basin and oceanic-ridge basalts. Earth Planet. Sci. Lett., 28: 299-307.

Rebay G. and Powell R., 2002. The formation of eclogite facies metatroctolites and a general petrogenetic grid in Na_2O-CaO-FeO-MgO-Al_2O_3-SiO_2-H_2O (NCFMASH). J. Metam. Geol., 20: 813-826.

Reed M.H., 1983. Seawater-basalt reaction and the origin of greenstones and related ore deposits. Econ. Geol., 78 (3): 466-485.

Reinecke T., 1982. Cymrite and celsian in manganese-rich metamorphic rocks from Andros island, Greece. Contrib. Mineral. Petrol., 79: 333-336.

Reinecke T., 1998. Prograde high- to ultrahigh-pressure metamorphism and exhumation of oceanic sediments at Lago di Cignana, Zermatt-Saas zone, Western Alps. Lithos, 42: 147-189.

Staudigel H., Planck T., White B. and Schmincke H.-U., 1996. Geochemical fluxes during seafloor alteration of the basaltic upper oceanic crust: DSDP site 417 and 418, AGU Geophys. Monogr., 96: 19-37.

Tartarotti P., 1988. Le ofioliti piemontesi nella media e bassa valle di St. Marcel (Aosta). Tesi Dott., Univ. Padova, 167 pp.

Tartarotti P. and Caucia F., 1993. Coexisting cummingtonite - sodic amphibole pair in metaquartzites from the ophiolites sedimentary cover (St. Marcel Valley, Italian Western Alps): a X-ray structure refinement and petrology study. N. Jahrb. Mineral. Abhandl., 165: 223-243.

Tartarotti P., Martin S. and Polino R., 1986. Geological data about the ophiolitic sequences in the St. Marcel Valley (Aosta Valley). Ofioliti, 11 (3): 343-346.

Tumiati S., 2005. Geochemistry, mineralogy and petrology of the eclogitised manganese deposit of Praborna (Valle d'Aosta, Western Italian Alps). PhD thesis, Univ. Insubria - Univ. Paris 7, 235 pp.

Tumiati S., Casartelli P., Mambretti A., Martin S., Frizzo P. and Rottoli M., 2005. The ancient mine of Servette (Saint-Marcel, Val d'Aosta, Western Italian Alps): a mineralogical, metallurgical and charcoal analysis of furnace slags. Archeometry, 47 (2): 317-340.

van der Klauw S.N.G.C., Reinecke T. and Stockhert B., 1997. Exhumation of ultrahigh-pressure metamorphic oceanic crust from Lago di Cignana, Piemontese zone, western Alps: the structural record in metabasites. Lithos, 41: 79-102.

Venturelli G., Thorpe R.S. and Potts P.J., 1981. Rare earth and trace element characteristics of ophiolitic metabasalts from Alpine-Apennine belt. Earth Planet. Sci. Lett., 53: 109-123.

Wei C.J., Powell R. and Zhang L.F., 2003. Eclogites from the south Tianshan, NW China: petrological characteristic and calculated mineral equilibria in the Na_2O-CaO-FeO-MgO-Al_2O_3-SiO_2-H_2O system. J. Metam. Geol., 21: 163-179.

Widmer T., Ganguin J. and Thompson A.B., 2000. Ocean floor hydrothermal veins in eclogite facies rocks of the Zermatt-Saas zone, Switzerland. Schweiz. Mineral. Petrogr. Mitt., 80: 67-73.

Wiewiora A. and Weiss Z., 1990. Crystallochemical classifications of phyllosilicates based on the unified system of projection of chemical composition. II. The chlorite group. Clay Minerals, 25: 83-92.

Received, July 7, 2006
Accepted, January 1, 2008